Available online at www.sciencedirect.com
SCIENCE DIRECT®
Journal of Sound and Vibration 273 (2004) 201–218
JOURNAL OF SOUND AND VIBRATION
www.elsevier.com/locate/jsvi

# Eigensensitivity based optimal distribution of a viscoelastic damping layer for a flexible beam

Tae-Woo Kim, Ji-Hwan Kim*

*School of Mechanical and Aerospace Engineering, College of Engineering, Seoul National University, Seoul 151-742, South Korea*

Received 11 November 2002; accepted 17 April 2003

**Abstract**

In this paper, optimal distribution of a viscoelastic damping layer is sought for suppression of the transient vibration of a flexible beam. For the damping design, eigenvalues in the range of interest are taken as design criteria rather than the responses at a specific frequency. Two eigensensitivity based optimizing procedures are proposed, which are analogous to the pole placement technique and optimal control theory for dynamic system design. For the eigenanalysis of the structure with frequency-dependent material, Golla–Hughes–McTavish (GHM) model is used in expressing the viscoelastic material property and an approximate eigensolution is employed to avoid the intensity of iterative computation in the optimization process which is caused by additional degrees of freedom due to GHM modelling. Optimized partial coverage configurations are illustrated and compared to the full coverage configuration demonstrating the improved vibration characteristic of the optimally layered structure.


## 1. Introduction

When exposed to vibrations, the high polymeric molecular properties exhibited by the viscoelastic materials enhance the system damping, thereby realizing considerable dissipation of vibration energy. There are two ways of layer damping treatment using these materials: unconstrained and constrained configuration, where the vibratory energy is dissipated due to direct strains in the former case and predominantly shear strains in the latter [1]. The costs of materials and application processes are often lowest for the unconstrained treatment though it is somewhat inefficient from a weight point of view compared with the constrained treatment, noting the efficiency of the constrained treatment is achieved at some cost with respect to the

*Corresponding author. Tel.: +82-2-880-7383; fax: +82-2-887-2662.
*E-mail address:* jwhkim@snu.ac.kr (J.-H. Kim).

0022-460X/03/$ - see front matter 
doi:10.1016/S0022-460X(03)00479-6

difficulty of application and greater analytic difficulty. Viscoelastic damping layers for noise and vibration control of flexible structures are widely used in various engineering fields, and passive control like this has still an attractive alternative in terms of economy, simplicity and stability compared to the more modern vibration control measures such as active and semi-active control.

Modelling and analyzing of viscoelastic structures are difficult and cumbersome for their frequency- or time-dependent material property. Then, many researchers have focused mainly on frequency-domain design for maximum performance, say, adjusting frequency response characteristics: maximizing modal loss factors [2]; minimizing fixed-frequency forced responses [3]; minimizing resonance responses [4]. On the other hand, when it comes to suppressing the transient vibration due to disturbances like impulse, eigenvalues are more familiar and consistent design criteria for characterizing the dynamic performance in damping design, as such in the pole placement technique. As the frequency-dependent properties of viscoelastic materials lead to an non-linear eigenvalue problem, however, the eigenanalysis of viscoelastic systems becomes unconventional one. It can be done in two ways, iteratively or directly using available eigenanalysis algorithm by introducing additional degrees of freedom. The latter has been made possible by virtue of recent development of the models for the viscoelastic behavior such as Golla–Hughes–McTavish (GHM) model [5]. At the cost of drastic increase in the problem size, which is caused by introducing additional dissipative co-ordinates beside the original co-ordinates, GHM model yields to a second order differential equation with constant coefficient matrices that is familiar with structural dynamicists. Hence, it enables one to obtain not only eigensolutions from the typical form of the eigenvalue problems but also dynamic responses such as transient or frequency response easily using available algorithms.

In this paper, optimal thickness distribution of an unconstrained viscoelastic damping layer is sought for the transient vibration suppression by controlling some dominant eigenmodes. Due to the nature of their action, the performance of damping layers strongly depends on their placement with respect to structural vibration mode shapes. For example, an unconstrained layer produces the highest damping if placed at structural antinodes. In many practical applications, such as aeronautic and space structures, damping treatment is subject to a very careful consideration of weight economy. Since the partial coverage technique has the advantage of adding less weight, efforts should be, therefore, made to find its optimal use. To this end, eigensensitivity based optimization procedure is proposed, which is analogous to that of pole placement technique and optimal control. In the first place, minimum mass configuration of the damping material is sought which satisfies constraints on the eigenvalues of some dominant modes for the dynamic requirements. Alternatively, the modified version of the performance index used in the optimal control theory is taken as the objective function, for there are no control forces, under constraints on the amount of the damping material. The damping treatment is allowed on both top and bottom of the structure and the results are compared with those for the one-sided full coverage case.

## 2. Finite element formulation

### 2.1. Governing equation

In Fig. 1, the geometric configuration of a cantilever beam, treated with unconstrained viscoelastic material, is illustrated, where only the base beam is clamped. There are two components:

the base beam and the viscoelastic layer—quantities associated with each of these components are denoted with superscript or subscript $b$ and $l$, respectively, throughout this paper. As shown in Fig. 2, the motion of points in the system is described using the lateral deflection $w$, the longitudinal displacement at the neutral axis of the base beam $u_0$, and the shear angle in the viscoelastic layer $\psi_y$, where the shear strain in the damping layer is considered for the cases that the layer is thick enough to cause considerable shear deformation, which may occur in partial coverage configurations.

The base beam is elastic and transverse shear strain is neglected. The lateral displacement of the middle of the base beam is shared by all points in the cross-section. The viscoelastic layer is lossy and the shear angle associated with non-negligible transverse shear is considered. The longitudinal normal strain in the viscoelastic layer is also included. Under these assumptions, the displacement fields are given by

$$\begin{aligned} u_b(x,z) &= u_0(x) - z\frac{\partial w(x)}{\partial x}, \\ u_l(x,z) &= u_0(x) - z\frac{\partial w(x)}{\partial x} - \left(z - \tfrac{1}{2}h_b\right)\psi_y(x), \end{aligned} \tag{1}$$

where the subscript 0 denotes the centerline of the base beam.

Now that the displacement of any point in the beam and the viscoelastic layer have been defined, the longitudinal normal and transverse shear strains may be determined as

$$\begin{aligned} \varepsilon_{xx}^b(x,z) &= \frac{\partial u_0(x)}{\partial x} - z\frac{\partial^2 w(x)}{\partial x^2}, \\ \varepsilon_{xx}^l(x,z) &= \frac{\partial u_0(x)}{\partial x} - z\frac{\partial^2 w(x)}{\partial x^2} - \left(z - \tfrac{1}{2}h_b\right)\frac{\partial \psi_y(x)}{\partial x}, \\ \gamma_{xz}^l(x,z) &= -\psi_y(x). \end{aligned} \tag{2}$$

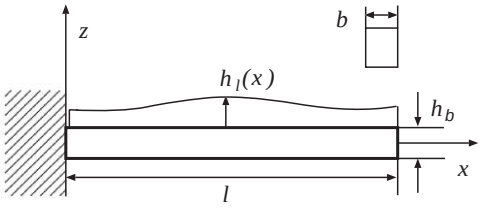


Fig. 1. Schematic diagram of a cantilever beam treated with a damping layer.

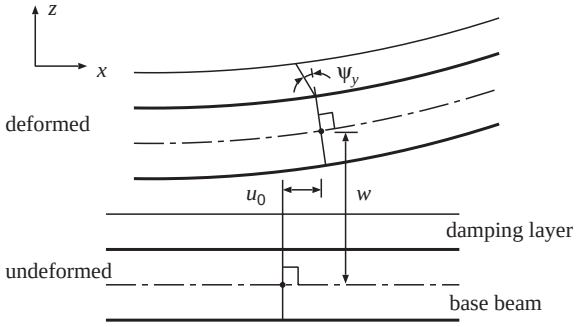


Fig. 2. Displacement fields.

In addition to the elastic constitutive equation of the base beam, linear viscoelastic constitutive equation of the layer is expressed in the convolution or hereditary integral form

$$\sigma_{xz}^{l}(t) = \int_0^t g(t-\tau)\frac{\partial \gamma_{xz}^{l}(\tau)}{\partial \tau}\,\mathrm{d}\tau, \tag{3}$$

where $g$ is the relaxation function. Through the Laplace transformation, the equation given above is transformed to

$$\tilde{\sigma}_{xz}^{l}(s) = s\tilde{g}(s)\tilde{\gamma}_{xz}^{l}(s) = G(s)\tilde{\gamma}_{xz}^{l}(s), \tag{4}$$

where $G(s)$ means complex modulus in case of $s = \mathrm{j}\omega$.

From the extended Hamilton's principle, one obtains the following equation composed of variation of the kinetic energy $\delta T$, the virtual internal energy $\delta U$ and the virtual work $\delta W$ done by external forces acted on the system,

$$\delta T - \delta U = \delta W. \tag{5}$$

Each term in the left-hand side of the equation above is expressed as

$$\begin{aligned}
\delta T &= \delta T_b + \delta T_l \\
&= b\int_0^l \left\{ \int_{-\frac{1}{2}h_b}^{\frac{1}{2}h_b} \rho_b(\dot{u}_b\delta\dot{u}_b + \dot{w}\delta\dot{w})\,\mathrm{d}z + \int_{\frac{1}{2}h_b}^{\frac{1}{2}h_b+h_l(x)} \rho_l(\dot{u}_l\delta\dot{u}_l + \dot{w}\delta\dot{w})\,\mathrm{d}z \right\}\mathrm{d}x \\
\delta U &= \delta U_b + \delta U_l \\
&= b\int_0^l \left\{ \int_{-\frac{1}{2}h_b}^{\frac{1}{2}h_b} \sigma_{xx}^{b}\delta\varepsilon_{xx}^{b}\,\mathrm{d}z + \int_{\frac{1}{2}h_b}^{\frac{1}{2}h_b+h_l(x)} (\sigma_{xx}^{l}\delta\varepsilon_{xx}^{l} + \sigma_{xz}^{l}\delta\gamma_{xz}^{l})\,\mathrm{d}z \right\}\mathrm{d}x,
\end{aligned} \tag{6}$$

where $\rho$ denotes material density.

### 2.2. Discretized equation

Discretized governing equation is obtained by substituting Eqs. (1)–(3) into Eq. (5) and interpolating $u_0$, $w$, $\psi$ by appropriate interpolation functions. In this paper, $w$ is interpolated using Hermitian elements which allow element-to-element continuity of deflection and slope. Also, $u_0$ is interpolated using a quadratic polynomial and $\psi$ is interpolated consistent with $u_0$ and $\partial w/\partial x$. Because slope and longitudinal displacement have the same interpolation order, the element will not shear lock [6].

Denoting mass matrix, stiffness matrix of the base beam, stiffness coefficient matrix of the layer, general displacement vector and external force vector as $\mathbf{M}$, $\mathbf{K}_b$, $\mathbf{K}_l$, $\mathbf{x}$ and $\mathbf{f}$, respectively, discretized equations are written as

$$\mathbf{M}\ddot{\mathbf{x}}(t) + \mathbf{K}_b\mathbf{x}(t) + \int_0^t g(t-\tau)\mathbf{K}_l\dot{\mathbf{x}}(\tau)\,\mathrm{d}\tau = \mathbf{f}(t). \tag{7}$$

From this equation, if the initial conditions are assumed to be zeros for convenience, one obtains the form in the Laplace domain

$$(s^2\mathbf{M} + \mathbf{K}_b + G(s)\mathbf{K}_l)\tilde{\mathbf{x}}(s) = \tilde{\mathbf{f}}(s). \tag{8}$$

## 3. Viscoelastic analysis

The frequency- or time-dependent behavior of the viscoelastic material can be captured by $G(s)$ in Eq. (8), which is obtained by curve fitting of the measured data. While $G(s)$ is linearly dependent on $s$ in viscously damped system, it is a non-linear function of $s$ and makes the eigenvalue problem non-linear in general viscoelastic systems. To describe the behavior of $G(s)$, various models have been developed based on spring-dashpot model [7], fractional calculus [8], Prony series [9], etc. Among others GHM model is used in this paper, for it renders the non-linear eigenvalue problem formulated to corresponding linear one and accounts for transient response.

### 3.1. GHM model

In this approach, the material modulus function is represented as a series of 'mini-oscillator' terms. Denoting that the factor $G^\infty$ is the value of the relaxation function $g(t)$ at $t = \infty$, $G(s)$ is expressed in the form

$$G(s) = G^\infty\left(1 + \sum_k \alpha_k \frac{s^2 + 2\hat{\zeta}_k\hat{\omega}_k s}{s^2 + 2\hat{\zeta}_k\hat{\omega}_k s + \hat{\omega}_k^2}\right), \tag{9}$$

where $\alpha_k$, $\hat{\zeta}_k$ and $\hat{\omega}_k$ are constants determined by curve fitting of the measured data.

The second order matrix equations of motion, which are most familiar form to structural dynamicists, are yielded by introducing auxiliary co-ordinates, called dissipation co-ordinates, of the form

$$\tilde{\mathbf{q}}_k(s) = \frac{\hat{\omega}_k^2}{s^2 + 2\hat{\zeta}_k\hat{\omega}_k s + \hat{\omega}_k^2}\tilde{\mathbf{x}}(s). \tag{10}$$

By substituting Eqs. (9) and (10) into Eq. (8) and inverse transformation, one obtains the following second order form equation with constant coefficient matrices:

$$\mathbf{M}_a\ddot{\mathbf{x}}_a(t) + \mathbf{C}_a\dot{\mathbf{x}}_a(t) + \mathbf{K}_a\mathbf{x}_a(t) = \mathbf{f}_a(t), \tag{11}$$

where each vector and matrix are expressed in case of $k = 2$ as

$$\mathbf{x}_a(t) = \begin{bmatrix} \mathbf{x}(t) \\ \mathbf{q}_1(t) \\ \mathbf{q}_2(t) \end{bmatrix}, \quad \mathbf{M}_a = \begin{bmatrix} \mathbf{M} & 0 & 0 \\ 0 & G^\infty\alpha_1\dfrac{1}{\hat{\omega}_1^2}\mathbf{K}_l & 0 \\ 0 & 0 & G^\infty\alpha_2\dfrac{1}{\hat{\omega}_2^2}\mathbf{K}_l \end{bmatrix},$$

$$\mathbf{C}_a = \begin{bmatrix} 0 & 0 & 0 \\ 0 & G^\infty \alpha_1 \dfrac{2\hat{\zeta}_1}{\hat{\omega}_1^2}\mathbf{K}_l & 0 \\ 0 & 0 & G^\infty \alpha_2 \dfrac{2\hat{\zeta}_2}{\hat{\omega}_2^2}\mathbf{K}_l \end{bmatrix},$$

$$\mathbf{K}_a = \begin{bmatrix} \mathbf{K}_b + G^\infty(1+\alpha_1)\mathbf{K}_l & -G^\infty\alpha_1\mathbf{K}_l & -G^\infty\alpha_2\mathbf{K}_l \\ -G^\infty\alpha_1\mathbf{K}_l & G^\infty\alpha_1\mathbf{K}_l & 0 \\ -G^\infty\alpha_2\mathbf{K}_l & 0 & G^\infty\alpha_2\mathbf{K}_l \end{bmatrix}, \quad \mathbf{f}_a(t) = \begin{bmatrix} \mathbf{f}(t) \\ 0 \\ 0 \end{bmatrix}$$

and more detailed derivations of this equation are found in Ref. [5]. It is to be noted that the size of matrix comes to be $k+1$ times as large as the original size. Namely, if the damping is modelled using the GHM model, the degree of freedom (d.o.f) is at least doubled.

### 3.2. Eigenvalue problem

The eigenvalue problem of Eq. (11) is to be dealt in the state space because the damping matrix $\mathbf{C}_a$ is non-proportional. Then, one can obtain straightforward the form with respect to $i$th mode

$$\mathbf{A}\mathbf{z}_i = \lambda_i \mathbf{B}\mathbf{z}_i, \tag{12}$$

where $\lambda_i$ is the $i$th eigenvalue and $\mathbf{A}$, $\mathbf{B}$, $\mathbf{z}_i$ are defined by

$$\mathbf{A} = \begin{bmatrix} -\mathbf{K}_a & 0 \\ 0 & \mathbf{M}_a \end{bmatrix}, \qquad \mathbf{B} = \begin{bmatrix} \mathbf{C}_a & \mathbf{M}_a \\ \mathbf{M}_a & 0 \end{bmatrix}, \qquad \mathbf{z}_i = \begin{bmatrix} \mathbf{q}_i \\ \lambda\mathbf{q}_i \end{bmatrix}.$$

The biggest drawback with this approach is the size of the matrix, and hence the computational effort required for the eigensolution. If d.o.f. of Eq. (7) is $n$, the number of the eigenvalues is $2n(k+1)$, which consists of, in lightly damped viscoelastic systems, $2n$ underdamped modes and $2nk$ overdamped modes [9,10]. To avoid the intensity of the computation in solving the eigenvalue problem of Eq. (12), an approximate method is employed which uses elastic modes, and applies under light damping assumption [11]. The corresponding elastic eigenmode is obtained by taking only constant part of $G(s)$ in dealing with Eq. (8). Namely, denoting that $\bar{\lambda}_i$ and $\bar{\mathbf{x}}_i$ is the $i$th elastic eigensolution pair, it satisfies the following equations normalized with respect to the mass matrix $\mathbf{M}$:

$$\{\bar{\lambda}_i^2\mathbf{M} + \mathbf{K}_b + G_c\mathbf{K}_l\}\bar{\mathbf{x}}_i = 0, \tag{13}$$

$$\bar{\mathbf{x}}_i^{\mathrm{T}}\mathbf{M}\bar{\mathbf{x}}_i = 1, \tag{14}$$

where

$$G_c = G^\infty\left(1 + \sum_k \alpha_k\right).$$

Now, consider a solution of the form

$$\mathbf{x}_i = \sum_{p=1}^{n} a_p \mathbf{x}_p, \tag{15}$$

where $a_i = 1$, $|a_p| \ll 1$ $(p \neq i)$ for small damping.

Then, using orthogonality of the undamped modes, one obtains the following by substituting Eq. (15) into the eigenvalue problem of Eq. (8) and multiplying on the left by transpose of $\bar{\mathbf{x}}_i$:

$$\lambda_i^2 + \sum_{p} G_s^{ip}(\lambda_i) a_p - \bar{\lambda}_i^2 = 0, \tag{16}$$

where, denoting the $s$-dependent part of $G(s)$ as $G_s(s)$,

$$G_s^{ip}(\lambda_i) = G_s(\lambda_i) \bar{\mathbf{x}}_i^{\mathrm{T}} \mathbf{K}_l \bar{\mathbf{x}}_p.$$

By neglecting small terms according to the assumption on the magnitude of $a_p$, Eq. (16) yields to

$$\lambda_i^2 + G_s^{ii}(\lambda_i) - \bar{\lambda}_i^2 \approx 0, \tag{17}$$

where the repeated index does not mean summation on $i$.

For the function $G_s(s)$ varies slowly with frequency for the material with normal damping mechanism, it is sufficient to evaluate the function at the undamped eigenvalue $\bar{\lambda}_i$. Considering that small damping also indicates small magnitude of the function $G_s(s)$, the $i$th underdamped mode is approximated based on Eq. (17) by

$$\lambda_i \approx \pm \bar{\lambda}_i - \frac{1}{2\bar{\lambda}_i} G_s^{ii}(\bar{\lambda}_i). \tag{18}$$

Also, the corresponding mode vector is written as

$$\mathbf{x}_i \approx \bar{\mathbf{x}}_i + \sum_{p \neq i} \frac{G_s^{pi}(\bar{\lambda}_i)}{(\bar{\lambda}_i^2 - \bar{\lambda}_p^2)} \bar{\mathbf{x}}_p, \tag{19}$$

where the coefficients $a_p$ $(p \neq i)$ are derived by substituting Eq. (15) into the eigenvalue problem of Eq. (8) and multiplying on the left by transpose of $\bar{\mathbf{x}}_p$ instead of $\bar{\mathbf{x}}_i$ to be

$$a_p \approx \frac{G_s^{pi}(\bar{\lambda}_i)}{(\bar{\lambda}_i^2 - \bar{\lambda}_p^2)}.$$

While the material modulus may be obtained from the measured modulus by using any suitable fitting function without producing GHM model of the material, the GHM expression is used to enable the comparison of the methods.

## 4. Optimization procedure

In this section, optimization is carried out in the aspect of improving the transient vibration characteristics of a flexible beam. Based on the method outlined above, eigenvalues of the system are taken as main design criteria for this passive damping design, for which many researches have been performed concerning about mainly the response at a specific frequency. For consistency, it

is attempted to hire optimization framework used for general dynamic system design methodologies such as the pole placement technique and optimal control theory [12].

### 4.1. Design parameter

The damping layer is treated on one side or both sides of the base beam and the thickness distribution of the layer is described by the linear interpolation between nodal points of the layer with upper and lower limits (see Fig. 3) [13]. The height at each nodal point, independent of the nodes for beam elements, is a design variable. In order to allow for steep slopes, design variables may become negative. For the numerical stability, eliminating elements is avoided by introducing a lower limit on the layer thickness. An upper limit is also imposed so that the analysis makes sense under prescribed fundamental assumptions in Section 2.1. It is to be noted that high enough order integration is required to capture the thickness variation in the beam element correctly where the integration is evaluated.

### 4.2. Objective function and constraint

Some of the lowest underdamped modes, rather than the overdamped ones, are taken into account since the former is more dominant than the latter in characterizing the vibration properties of the system. The optimization problem is presented in two ways described below. First, the minimum mass configuration of the thickness distribution is sought with constraints on real and imaginary parts of the considered eigenmodes, which is analogous to the pole placement technique. This statement is expressed in the mathematical form

$$\begin{aligned} &\text{minimize} && \rho_l b \int_0^l h_l(x)\mathrm{d}x \\ &\text{subject to} && f_R^i\{\Re(\lambda_i)\} \leqslant 0, \\ & && f_I^i\{\Im(\lambda_i)\} \leqslant 0 \quad (i = 1, \ldots, m), \end{aligned} \tag{20}$$

where $f_R^i$ and $f_I^i$ are constraint functions for real and imaginary parts of the $i$th eigenvalue respectively, and $m$ is the number of modes to be included in the analysis. However, convergence of this optimization process is not always guaranteed, for the sensitivity of each mode with respect to the design parameter is not independent, and even real and imaginary values of a mode neither. In other words, because the variance of mass, stiffness and damping property of the system are related one another by the material property of the added damping layer, sensitivities of the

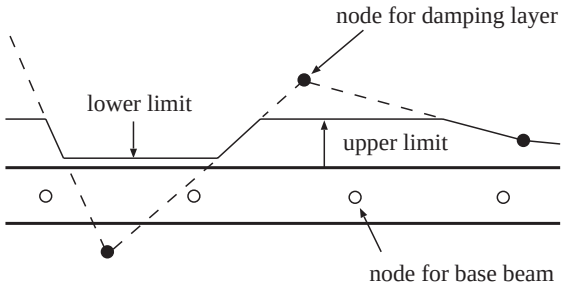


Fig. 3. Design parameters for thickness distribution of the damping layer.

constraint functions are coupled one another and the optimal location for one mode affects the case of the other modes. In addition, the limited amount of the damping material provides another design constraint. Therefore, one must be careful in setting boundary values on the constraints.

Alternatively, a performance index is defined as the objective function that is analogous to the one used in the optimal control theory. Consisting of the weighted sum of the modal potential and kinetic energy accumulated till the vibration of the system dies out, it brings state variables to the equilibrium state as fast as possible in terms of energy minimization. Since there are no control forces, the optimal thickness distribution is sought under a constraint on the mass of the damping layer. Then, in the mathematical form, the second optimization problem is written as

$$\begin{aligned} &\text{minimize} \quad P = \int_0^\infty \sum_{i=1}^{m} \{c_i \eta_i^2(t) + d_i \dot{\eta}_i^2(t)\}\, \mathrm{d}t \\ &\text{subject to} \quad bl \int_{\frac{1}{2}h_b}^{\frac{1}{2}h_b + h_l(x)} \rho_l \, \mathrm{d}x - \hat{m} \leqslant 0, \end{aligned} \tag{21}$$

where $\eta_i(t)$ is the $i$th mode response and $c_i$ and $d_i$ are weighting factors and $\hat{m}$ is a given amount of the damping material.

If each modal response is considered as the solution of one degree of freedom spring-dashpot underdamped vibration, the $i$th modal response can be written in terms of $i$th natural frequency $\omega_i$ and damping ratio $\zeta_i$ as

$$\eta_i(t) = A_i \mathrm{e}^{-\zeta_i \omega_i} \sin(\omega_i \sqrt{1-\zeta_i^2} + \theta_i), \tag{22}$$

where

$$A_i = \frac{\sqrt{\{\dot{\eta}_i(0) + \zeta_i \eta_i(0)\}^2 + \eta_i^2(0)\omega_i^2(1-\zeta_i^2)}}{\omega_i^2(1-\zeta_i^2)}, \quad \theta_i = \arctan \frac{\eta_i(0)\omega_i\sqrt{1-\zeta_i^2}}{\dot{\eta}_i(0) + \zeta_i \omega_i \eta_i(0)}.$$

Substituting Eq. (22) into the index $P$ and evaluating the integration, the performance index is written as

$$P = \sum_{i=1}^{m} \eta_i^2(0) \left[ c_i \left\{ \frac{1}{4\zeta_i \omega_i^3} \left( \frac{\dot{\eta}_i(0)}{\eta_i(0)} + 2\zeta_i \omega_i \right)^2 + \frac{1}{4\zeta_i \omega_i} \right\} + d_i \left\{ \frac{1}{4\zeta_i \omega_i} \left( \frac{\dot{\eta}_i(0)}{\eta_i(0)} \right)^2 + \frac{\omega_i}{4\zeta_i} \right\} \right]. \tag{23}$$

As one can see, the index is dependent on the initial conditions, and thus the optimal thickness distribution comes to be subject to them. To obtain the consistent form, independent of initial conditions, the minimum values of each braced term are taken as the objective parameters to be minimized instead. Then, the modified version of Eq. (21) is written as

$$\begin{aligned} &\text{minimize} \quad \bar{P} = \sum_{i=1}^{m} \left( \bar{c}_i \frac{1}{\zeta_i \omega_i} + \bar{d}_i \frac{\omega_i}{\zeta_i} \right) \\ &\text{subject to} \quad \rho_l b \int_0^l h_l(x)\, \mathrm{d}x - \hat{m} \leqslant 0, \end{aligned} \tag{24}$$

where $\bar{c}_i$ and $\bar{d}_i$ are weighting factors. Furthermore, it is possible to write Eq. (24) in terms of real and imaginary parts of the $i$th eigenvalue using following equations:

$$\Re(\lambda_i) = -\zeta_i\omega_i, \quad \Im(\lambda_i) = \omega_i\sqrt{1-\zeta_i^2}. \tag{25}$$

### 4.3. Eigenvalue sensitivity

From Eq. (12) eigenvalue sensitivity is calculated by differentiating both sides with respect to a design parameter $p$ and using symmetric property of $\mathbf{A}$ and $\mathbf{B}$ as [14]

$$\frac{\partial\lambda_i}{\partial p} = \frac{\mathbf{z}_i^{\mathrm{T}}(\partial\mathbf{A}/\partial p - \lambda_i\partial\mathbf{B}/\partial p)\mathbf{z}_i}{\mathbf{z}_i^{\mathrm{T}}\mathbf{B}\mathbf{z}_i} \tag{26}$$

If eigensolutions happen to be obtained through certain methods such as the approximate solution discussed in Section 3.2, the sensitivity can be given from Eq. (8) directly without formulation in the state-space following the analysis mentioned in deriving Eq. (26) closely:

$$\frac{\partial\lambda_i}{\partial p} = -\frac{\mathbf{x}_i^{\mathrm{T}}\{\lambda_i^2\partial\mathbf{M}/\partial p + G(\lambda_i)\partial\mathbf{K}_l/\partial p\}\mathbf{x}_i}{\mathbf{x}_i^{\mathrm{T}}\{2\lambda_i\mathbf{M} + (\partial G(\lambda_i)/\partial\lambda_i)\mathbf{K}_l\}\mathbf{x}_i}. \tag{27}$$

## 5. Results and discussion

Table 1 shows the material property and geometric dimension used in the numerical analysis. Viscoelastic material property is expressed by the GHM model with two second order terms ($k = 2$) [15]. Cares must be taken for the analysis to be within the frequency range of the GHM model. For the non-linear constrained minimization problems of Eqs. (20) and (24), 'constr' command in MATLAB is used, which applies the sequential quadratic programming with the quasi-Newton gradient search method. Each beam node has four d.o.f.—axial displacement $u_0$, transverse displacement $w$, rotation angle $\partial w/\partial x$ of the base beam and shear angle of the layer $\psi_y$. And two internal nodes, related to the axial displacement and shear angle, are embedded in each beam element. If two second order terms are required to successfully fit the viscoelastic material properties, then the number of d.o.f. is three times as many as that of physical d.o.f., even up to six times in case of state-space transformation, and results in drastic increase in the computational efforts for the eigensolution. Therefore, the approximate eigensolution is adopted for the iteration process to lighten the computational efforts and the GHM based solution is applied in the final converged configuration only. To show the validity of the approximate solution for the damping level that is to be tested, some comparison works are done between the solutions from Eqs. (12) and (18). Table 2 shows natural frequencies and damping ratios of the three lowest modes calculated through the former and the latter equation, respectively, where the beam has 10 elements and the damping layer is treated fully with the thickness of the base beam on both sides of the beam. One can notice that the approximate solution of the second mode, which shows the highest damping ratio among those three, does not follow the GHM solution well unlike those of two other modes. That is due to the increased contribution of the other modes ($p \neq i$) in the approximate solution Eq. (15). Therefore, the numerical analysis detailed below is carried out

Table 1
Material and geometric data

| | | |
|---|---|---|
| *Base beam* (*Al*) | | |
| Length 1 m | Width 0.01 m | Thickness 0.005 m |
| Density 2700 kg/m$^3$ | Young's modulus 70 GPa | |
| *Damping layer* (*DYAD-606 Soundcoat*, 25°C) | | |
| Density 1105 kg/m$^3$ | The Poisson ratio 0.49 | $G^{\infty}$ 1.18 MPa |
| $\hat{\alpha}_1$ 87.5 | $\hat{\zeta}_1$ 1344.6 | $\hat{\omega}_1$ 1494.5 |
| $\hat{\alpha}_2$ 263.1 | $\hat{\zeta}_2$ 129.6 | $\hat{\omega}_2$ 39999.9 |

Table 2
Validity of the approximate solution compared to the GHM solution

| Mode | | 1st | 2nd | 3rd |
|---|---|---|---|---|
| Natural frequency (rad/s) | GHM | 20.3 | 135.6 | 400.6 |
| | Approx. | 20.5 | 136.1 | 399.9 |
| Damping ratio | GHM | 0.0212 | 0.0716 | 0.0415 |
| | Approx. | 0.0204 | 0.0624 | 0.0395 |

within tolerance of discrepancy between the two solutions considering the damping level of the tested models.

The damping material is allowed to be layered on both sides of the base beam. The number of beam elements and design parameters used in the following examples are determined after convergence study to be 10 and 17, respectively. For the numerical stability and feasibility of the analysis, the lower limit and upper limit are set on the thickness of the layer, as $1 \times 10^{-7}$ and thickness of the base beam, respectively. As a reference model, the single-sided fully covered case is taken for the comparison, where the thickness of the layer is the same as that of the base beam.

### 5.1. Minimum mass

First, minimum mass configuration is sought satisfying required dynamic performance set by constraints on dominant eigenvalues of the structure. The real and imaginary parts of the considered modes are to be constrained, respectively, at the same time, for improving the property of the one may mean degrading that of the other such as too much damping lowers resonance frequency considerably. In this example, the upper boundary is imposed on the real part of the chosen mode for damping property and the lower boundary on the imaginary, considering positive one of a conjugate pair, for stiffness property. Then, constraints of Eq. (20) are expressed as

$$\begin{aligned} &\Re(\lambda_i) - \Re(\hat{\lambda}_i) \leqslant 0, \\ &-\Im(\lambda_i) + \Im(\hat{\lambda}_i) \leqslant 0 \quad (i = 1, \ldots, m), \end{aligned} \tag{28}$$

where $\hat{\lambda}_i$ is the specified $i$th eigenvalue. As the constraint functions, left-hand side of Eq. (28), are non-linear functions of design parameters and coupled one another, the more modes are considered in the analysis, the more difficult it becomes to find the feasible domain. Thus, it is of great importance in point of convergence to take appropriate initial values of the design parameters. The thickness distribution on one side (symmetric on the other side) is plotted in Fig. 4 for the following three constraint cases:

*Case* 1: Double-sided, first mode constrained;
*Case* 2: Double-sided, first and second modes constrained;
*Case* 3: Double-sided, first through third modes constrained;

where the real and imaginary parts of corresponding eigenvalues of the reference model are assigned to each boundary value of the constraints, and $r_m$ denotes mass ratio of present to reference case. It shows rather discrete than uniform or smooth configurations, which confirms the importance of appropriate placement of the damping layer. Fig. 5 shows the design domains for each mode eigenvalue and the locations of the updated eigenvalues are marked for each case in the upper half region of the complex plane. The considered eigenmodes in the optimization

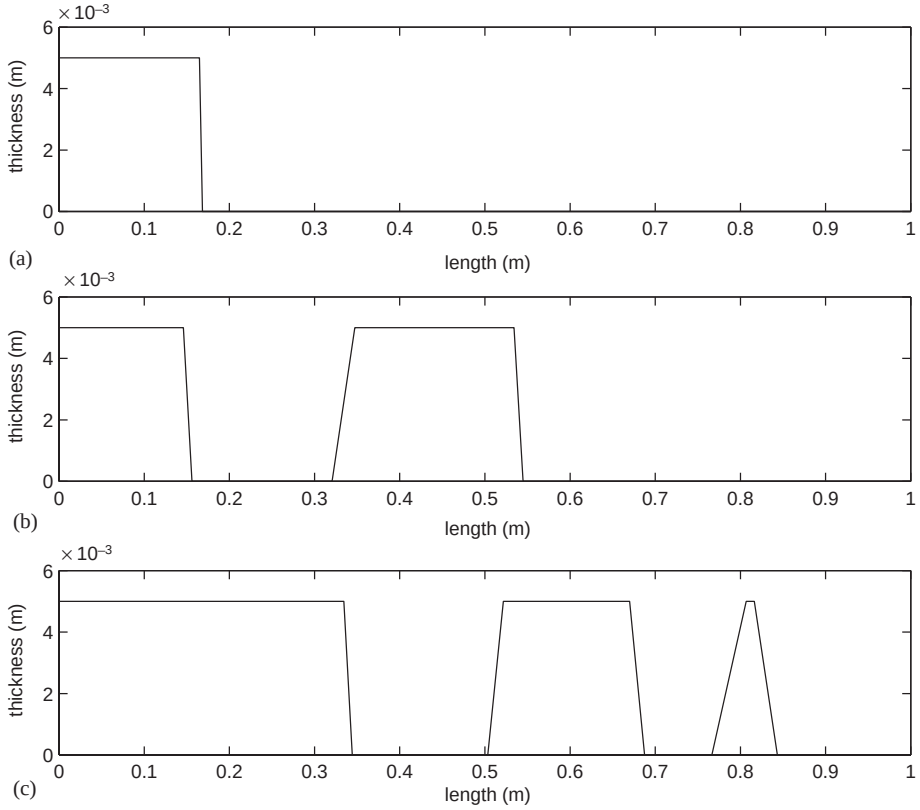


Fig. 4. Thickness distribution of the damping layer (symmetric on the other side): (a) case 1 ($r_m = 0.33$), (b) case 2 ($r_m = 0.72$), (c) case 3 ($r_m = 1.1$).

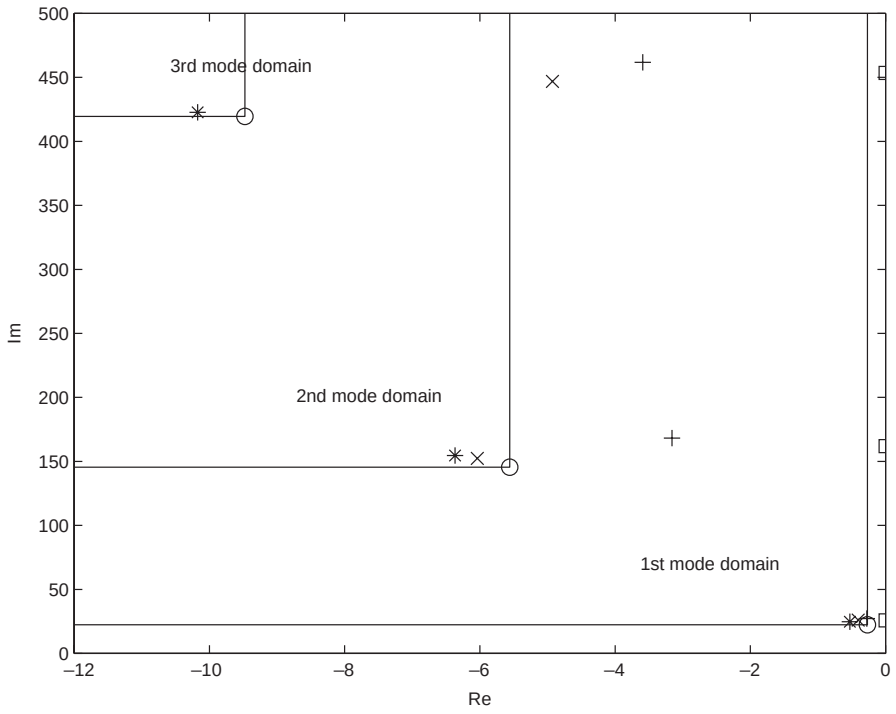


Fig. 5. Design domain and location of updated eigenvalues: □, untreated; ○, single-sided fully covered; +, case 1; ×, case 2; ∗, case 3.

process are placed in the target area as expected and one can notice that it may be achieved at the expense of the performance of the other modes, or increasing the real parts of the other modes compared to the reference. This situation is reflected in Fig. 6, which compares the frequency response for each coverage configuration, where the beam is forced at the tip and the response is measured at the same point. The response of each case is depicted using a solid line in (a), (b), (c), respectively, and the responses of the untreated beam and the reference model are superimposed using a dotted and dashed line for comparison. One finds the negative effect of the partial coverage on the unconsidered modes by increasing the magnitude at the resonant frequency. For the considered modes of each simulated case, the magnitudes at the resonant frequencies are found to be lowered while the resonant frequencies being prevented from being dropped too much compared to the reference, which means that the modification of damping and stiffness property is considered simultaneously by manipulating eigenvalues in this approach. Thus, it is noticed that the responses of the optimally layered beam in the lower frequency range due to increase of the lowest resonance frequency.

### 5.2. Maximum performance

Using the performance index defined in Eq. (24), optimization is carried out for three lowest underdamped modes with three different weighting cases $[\bar{c}_1\ \bar{c}_2\ \bar{c}_3\ \bar{d}_1\ \bar{d}_2\ \bar{d}_3]$ according to the

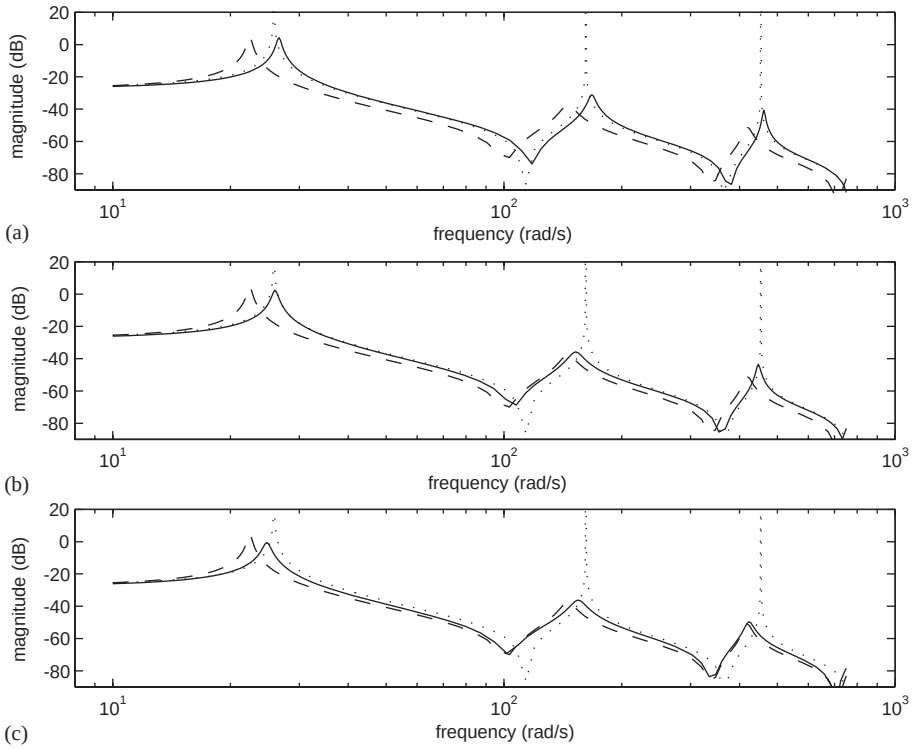


Fig. 6. Frequency response at the tip: ···, untreated; – –, single-sided fully covered. (a) case 1, (b) case 2, (c) case 3.

number of modes included in the optimization process:

*Case* 4: Double-sided, $[\omega_1^b \;\; 0 \;\; 0 \;\; 1/\omega_1^b \;\; 0 \;\; 0]$.
*Case* 5: Double-sided, $[\omega_1^b \;\; \omega_2^b \;\; 0 \;\; 1/\omega_1^b \;\; 1/\omega_2^b \;\; 0\,]$.
*Case* 6: Double-sided, $[\omega_1^b \;\; \omega_2^b \;\; \omega_3^b \;\; 1/\omega_1^b \;\; 1/\omega_2^b \;\; 1/\omega_3^b]$,

where $\omega_i^b$ $(i = 1, 2, 3)$ is natural frequency of the untreated base beam and the mass of the layer is constrained by that of the reference model. Optimized thickness distribution on one side (symmetric on the other side) is plotted in Fig. 7 for each weighting case. The same amount of damping material is distributed differently depending on the modes to be adjusted and shows that there seems to be no intermediate values, which implies that the location of the damping layer is to be closely investigated to control the property of certain modes effectively. All of three cases converge fast and well unlike the previous approach, for it is easy to find the feasible domain due to the simple constraint condition, mass of the damping layer. Fig. 8 shows the location of the updated eigenvalues marked for each case in the upper half region of the complex plane. Compared to the location of the eigenvalues of the reference model which has the same amount of the damping material as the tested cases, one can notice that improved eigenproperty is obtained for the considered modes—namely first mode of case 4, first and second modes of case 5, first

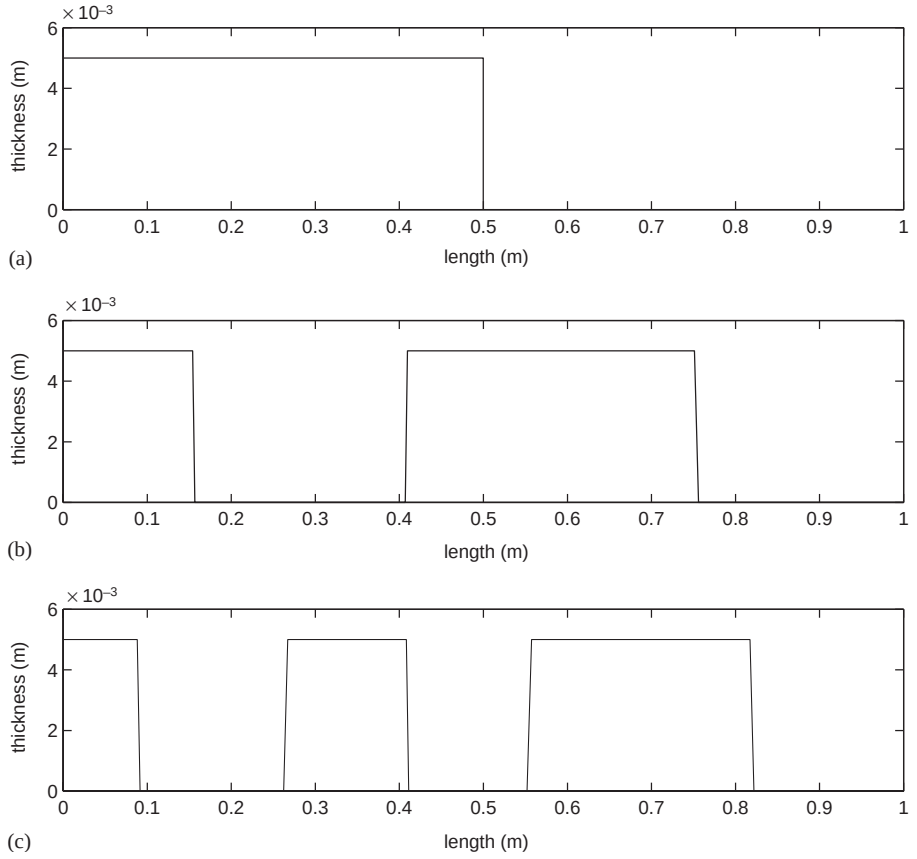


Fig. 7. Thickness distribution of the damping layer (symmetric on the other side): (a) case 4, (b) case 5, (c) case 6.

through third modes of case 6—in that they have higher natural frequency and damping ratio than the reference. The enhanced dynamic property is shown in Fig. 9, where the frequency responses are obtained under the same condition and plotted with the same legends as those for Fig. 6. The magnitude at the resonant frequency is found to be lowered and the resonant frequency to become higher than the reference values for the considered modes of each case, which means that better stiffness and damping property of the target mode are obtained by the optimization. The improved stiffness characteristic is evident in case 4 in contrast to the single-sided fully covered beam by noticing that the response in the lower frequency region is better than that of the untreated beam. In cases 5 and 6, each mode is weighted in a way that it has the same order of importance in these examples, and so one can obtain better results by putting more weights on the important modes. Considering that improving the dynamic behavior of any mode may cause the degradation of the other modes, there needs to be trade-offs among eigenproperty of the modes to be modified by co-ordinating weighting values.

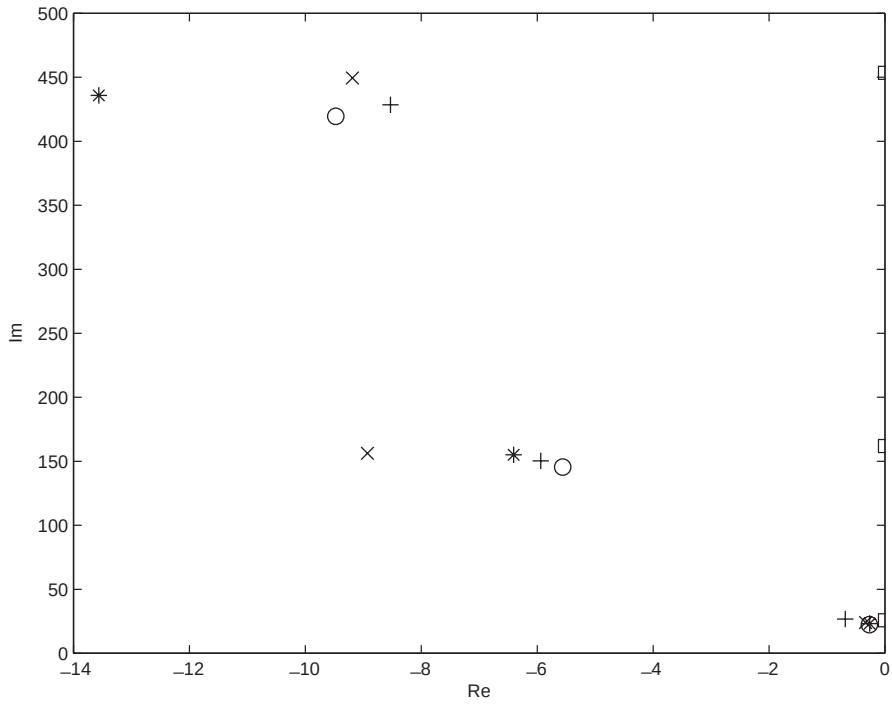


Fig. 8. Location of updated eigenvalues: □, untreated; ○, single-sided fully covered; +, case 4; ×, case 5; ∗, case 6.

## 6. Conclusion

This paper has considered optimal coverage of an unconstrained viscoelastic layer damping treatment for the transient vibration suppression of a flexible beam. In the proposed framework, two eigenvalue sensitivity based design procedures, which are analogies of the pole placement technique and optimal control theory for dynamic system design, were introduced. They were modified to be suitable for the passive damping design and numerical examples presented. Through the proposed optimization process, the enhanced dynamic property of the chosen modes was shown by frequency responses compared to that of the uniformly layered beam with the same amount of the damping layer. It was also shown that the layer is distributed rather discretely than smoothly gathering around certain positions depending on the considered modes. The proposed approaches consider the variation of stiffness and damping property due to the added damping material simultaneously, so that the stiffness reduction can be controlled to some extent. As far as the convergence is concerned, the index-based optimization shows better numerical performance than the one that constrains eigenmodes of interest. In a numerical point of view, fast iteration algorithm for the viscoelastically damped eigenvalue problems is essential in this approach, and the approximate solution used for the presented iteration process, under light damping assumption, is to be expanded in case of moderately damped viscoelastic structures that can be achieved by using the enhanced damping treatment such as constrained layer damping treatment.

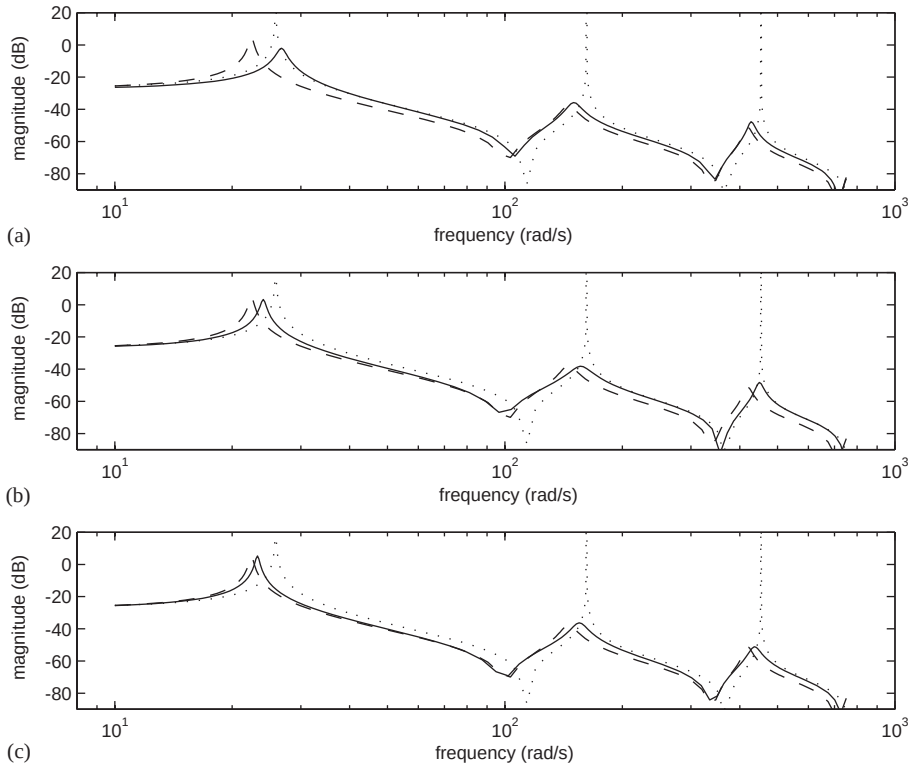


Fig. 9. Frequency response at the tip: ⋯, untreated; – –, single-sided fully covered. (a) case 4, (b) case 5, (c) case 6.

## References

[1] A.D. Nashif, D.I.G. Jones, J.P. Henderson, *Vibration Damping*, Wiley, New York, 1985.
[2] A. Yildiz, K. Stevens, Optimum thickness distribution of unconstrained viscoelastic damping layer treatments for plates, *Journal of Sound and Vibration* 103 (1985) 183–199.
[3] B.C. Nakra, Vibration control in machine and structures using viscoelastic damping, *Journal of Sound and Vibration* 211 (3) (1998) 449–465.
[4] R. Luden, Optimum distribution of additive damping for vibrating frames, *Journal of Sound and Vibration* 72 (1980) 391–409.
[5] D.J. McTavish, P.C. Hughes, Modeling of linear viscoelastic space structures, *Journal of Vibration and Acoustics* 115 (1993) 103–110.
[6] G.A. Lesieutre, U. Lee, A finite element for beams having segmented active constrained layers with frequency-dependent viscoelastics, *Smart Materials and Structures Journal* 5 (1996) 615–627.
[7] W. Flügge, *Viscoelasticity*, 2nd Revised Edition, Springer, Berlin, 1975.
[8] L.B. Eldred, W.P. Baker, A.N. Palazotto, Kelvin–Voigt vs fractional derivative model as constitutive relation for viscoelastic materials, *American Institute of Aeronautics and Astronautics Journal* 33 (3) (1995) 547–550.
[9] A. Muravyov, S.G. Hutton, Closed-form solutions and the eigenvalue problems for vibration of discrete viscoelastic systems, *Journal of Applied Mechanics* 64 (1997) 684–691.
[10] M.I. Friswell, D.J. Inman, Reduced-order models of structures with viscoelastic components, *American Institute of Aeronautics and Astronautics Journal* 37 (10) (1999) 1318–1325.

[11] J. Woodhouse, Linear damping model for structural vibration, *Journal of Sound and Vibration* 215 (3) (1998) 547–569.
[12] J.L. Junkins, Y. Kim, *Introduction to Dynamics and Control of Flexible Structures*, AIAA, New York, 1993.
[13] H.-W. Wodtke, J.S. Lamancusa, Sound power minimization of circular plates through damping layer placement, *Journal of Sound and Vibration* 215 (5) (1998) 1145–1163.
[14] R.T. Haftka, Z. Güdal, *Elements of Structural Optimization*, 3rd Revised and Expanded Edition, Kluwer Academic Publishers, Dordrecht, 1992.
[15] C.H. Park, D.J. Inman, M.J. Lam, Model reduction of viscoelastic finite element models, *Journal of Sound and Vibration* 219 (4) (1999) 619–637.